

2016 Spring Technical Meeting  
Central States Section of the Combustion Institute  
May 15-17, 2016  
Knoxville, Tennessee

## Correlation of normal gravity mixed convection blowoff limits with microgravity forced flow blowoff limits

*Jeremy W. Marcum<sup>1</sup>, Sandra L. Olson<sup>2\*</sup>, Paul V. Ferkul<sup>3</sup>*

*<sup>1</sup>University of Akron;*

*<sup>2</sup>NASA Glenn Research Center;*

*<sup>3</sup>USRA*

*\*Corresponding Author Email: Sandra.olson@nasa.gov*

**Abstract:** The axisymmetric rod geometry in upward axial stagnation flow provides a simple way to measure normal gravity blowoff limits to compare with microgravity Burning and Suppression of Solids – II (BASS-II) results recently obtained aboard the International Space Station. This testing utilized the same BASS-II concurrent rod geometry, but with the addition of normal gravity buoyant flow. Cast polymethylmethacrylate (PMMA) rods of diameters ranging from 0.635 cm to 3.81 cm were burned at oxygen concentrations ranging from 14 to 18% by volume. The forced flow velocity where blowoff occurred was determined for each rod size and oxygen concentration. These blowoff limits compare favorably with the BASS-II results when the buoyant stretch is included and the flow is corrected by considering the blockage factor of the fuel. From these results, the normal gravity blowoff boundary for this axisymmetric rod geometry is determined to be linear, with oxygen concentration directly proportional to flow speed. We describe a new normal gravity ‘upward flame spread test’ method which extrapolates the linear blowoff boundary to the zero stretch limit in order to resolve microgravity flammability limits—something current methods cannot do. This new test method can improve spacecraft fire safety for future exploration missions by providing a tractable way to obtain good estimates of material flammability in low gravity.

**Keywords:** *Blowoff, Axisymmetric, Stagnation, PMMA rod*

### 1. Introduction

Early work [1] on flammability limits has demonstrated that a hemispherical stagnation flow geometry is a good way to obtain the flammability limits of various fuels as a function of upward flowing oxidizer gas. Many heavier hydrocarbons were found to have similar limiting oxygen concentrations (13%-14%) and flame temperatures (1450-1500°C). The stagnation flow geometry is amenable to asymptotic analyses [2, 3], numerical modeling [4-6], and experimental extinction work for both axisymmetric and 2D geometries [7-11].

Recent testing completed on the International Space Station investigated the oxygen-flow flammability boundary for three different cast PMMA rod sizes [12]. This paper describes normal gravity tests conducted to complement the flight results.

## 2. Experimental

The test setup depicted in Figure 1 was used to determine the blowoff limit for cast PMMA rods having different radii. The apparatus consists of a flow system with two sources of gas; shop air and calibrated premixed bottles of 14% to 18% oxygen by volume in balance nitrogen. A manual valve selects the gas source. The gas flows through a 200 SLPM MKS mass flow controller and into a flow straightener, which provides a uniform flow profile, verified by hot wire anemometer profiling. The flow then enters the quartz tube, which has a 7.6 cm inside diameter and is 25.4 cm long. Matte black foil eliminates reflections from the back of the tube. A color video camera records each experiment through the clear tube. An exhaust snorkel above the tube removes combustion products from the lab.

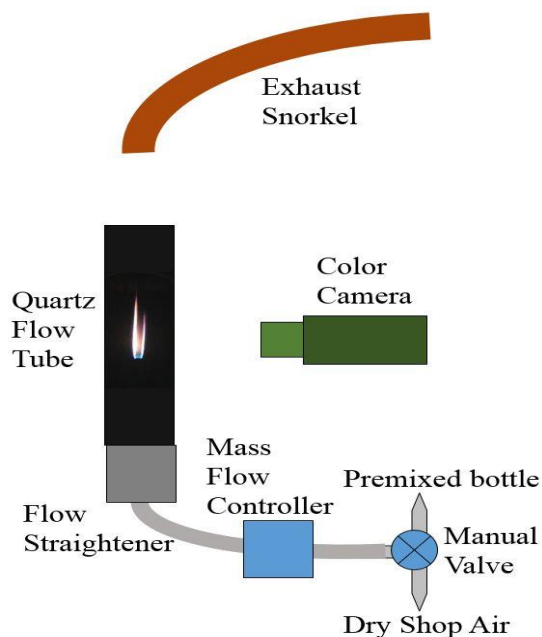


**Figure 1:** Test apparatus schematic. On/off valves, pressure regulators, and relief valves are not shown.

Each experiment begins by imaging a scale inside the tube next to the rod along with a card noting the test conditions. Dry shop air (dried using an O’Keefe air dryer) is set to the desired test flow rate on the mass flow controller. Each of the cast PMMA rods, hanging from a metal crossbar, were ignited manually outside of the apparatus and then suspended in the otherwise empty flow tube. Once the flame stabilized inside the tube, the gas source was switched from dry shop air to the premixed bottle test gas at the same flow rate to determine if the flame would blow off at that flow and oxygen combination. The lowest flow rate where blowoff occurs was determined iteratively for each oxygen concentration.

Due to limitations in system pressures, the maximum flow rate was 165 SLPM (60.3 cm/s average tube speed). This limited the range of oxygen concentrations where blowoff could be obtained.

Five radii of cast clear PMMA rods were tested; 0.318 cm, 0.476 cm, 0.635 cm, 1.270 cm, and 1.905 cm, spanning a factor of six in radius. Before determining the lowest blowoff limit at

each oxygen concentration, each initially flat-ended rod was allowed to burn to a rounded tip which is more representative of the steady-state shape of a burning sample.

### 3. Results

Over 280 experiments were conducted to determine the blowoff limits for each oxygen concentration and rod radius, and the bracketing flow conditions were repeated at least once. Figure 2 shows the flames just as blowoff begins at each limiting flow condition. Note that at 18% oxygen, blowoff limits are found at only three radii due to flow rate limitations.

From these images, some general trends are noted. Flame blowoff always occurs at the stagnation region. The triggering event appears to be the development of a flame hole [13] at the stagnation region of sufficient size to destabilize the flame base. Due to the destabilization, the flame blows downstream. The larger the radius, the larger the flame hole needs to be to destabilize the flame, which is consistent with reference 13 for flame holes in the presence of a heat sink. Small flame holes might disappear or be “healed,” but a subsequent larger hole can destabilize the flame and lead to blowoff. In some cases at higher oxygen and smaller radii, this downstream flame would briefly anchor to the sides of the rod, but then the anchor ring would begin to oscillate up and down with increasing amplitude until the flame invariably blew off.

Figure 3 presents the blowoff boundaries found for each rod radius in terms of oxygen concentration versus forced flow velocity. Each boundary is approximately linear with flow, with the exception of the 14% oxygen data, where all the data collapses at forced flow velocities less than 5 cm/s. This result is anomalous and explained as follows. At a sufficiently low forced flow rate, entrainment of air into the quartz tube from the top might be mixing with the supplied gas, increasing the ambient oxygen concentration so that the rod remained flammable.

To investigate this behavior, tests were repeated in the ZGRF wind tunnel rig [14] at the same normal gravity conditions of 14% O<sub>2</sub> and 2 cm/s flow. The wind tunnel rig provides a 20 cm diameter flow system with much less chance of entraining air from the top. Unlike in the 1g setup in the lab, the rod blew off in repeated tests at 14% oxygen in the larger wind tunnel as shown in Figure 4. A test was then repeated at 15% O<sub>2</sub> in the ZGRF wind tunnel to determine whether there was still an entrainment effect in the quartz tube data at the higher flow speeds. However, this flame did not blow off. Given these results, the 14% O<sub>2</sub> data are discarded from further analysis.

Figure 5 plots the blowoff forced stretch rate as a function of rod radius  $r$  for each oxygen concentration. The forced stretch rate is defined as  $a=3/2 U/r$ , where  $U$  is the average flow speed entering the tube and  $r$  is the rod radius. The data at each oxygen concentration is fitted with a power law having a square root exponent, which is attributed to the flame stretch at the flame standoff distance rather than the rod surface. The flame standoff distance is estimated using the gas phase thermal length scale, defined as  $\delta = (\alpha/a)^{1/2}$ , where  $\alpha$  is the gas phase thermal diffusivity and  $a$  is the stretch rate defined above. This length scale  $\delta$  is thus proportional to  $r^{1/2}$  for a given velocity  $U$ . In the inset, the coefficient  $C$  for each power law fit is plotted versus oxygen, revealing that the forced stretch rate at blowoff varies linearly with oxygen in addition to varying as the square root of the rod radius. These relationships guided the subsequent correlation of the data.

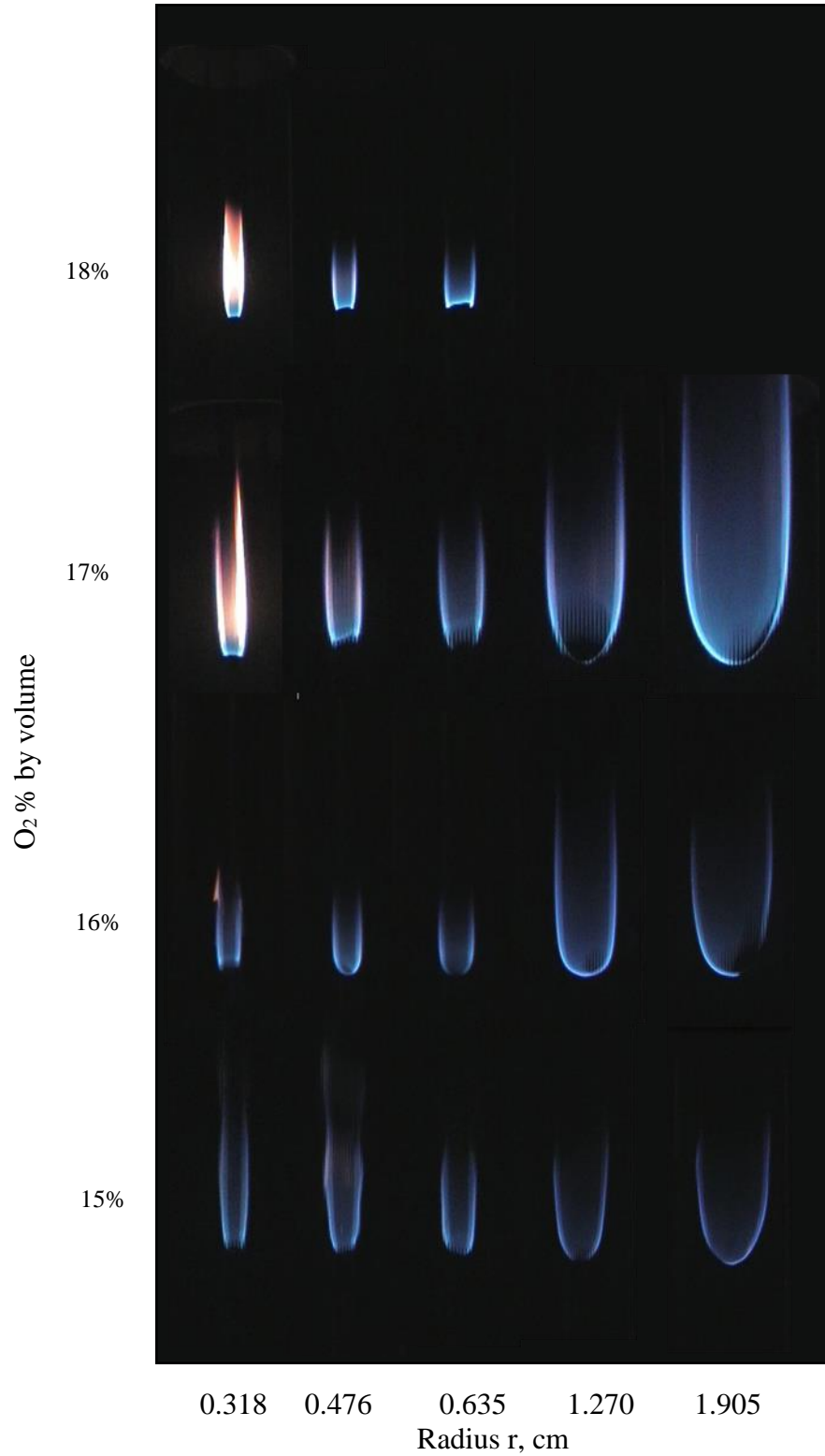


**Figure 2:** Flame images just before blowoff for each oxygen concentration and rod radius.

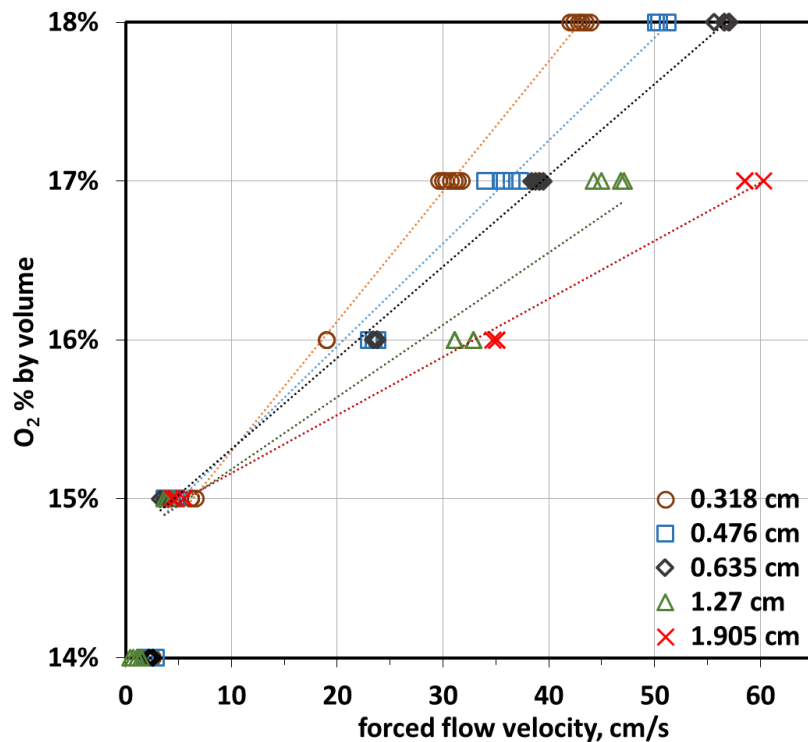


**Figure 3:** Blowoff boundaries for each rod radius as a function of oxygen concentration and forced flow velocity.



**Figure 4:** Non-symmetric flame in quartz tube at 14% oxygen, left, does not blowoff due to ambient flow entrainment back into the tube. Flame does blow off in larger wind tunnel, right, at 14% oxygen and 2 cm/s forced flow. Note: camera systems are not the same, although images are approximately to scale.

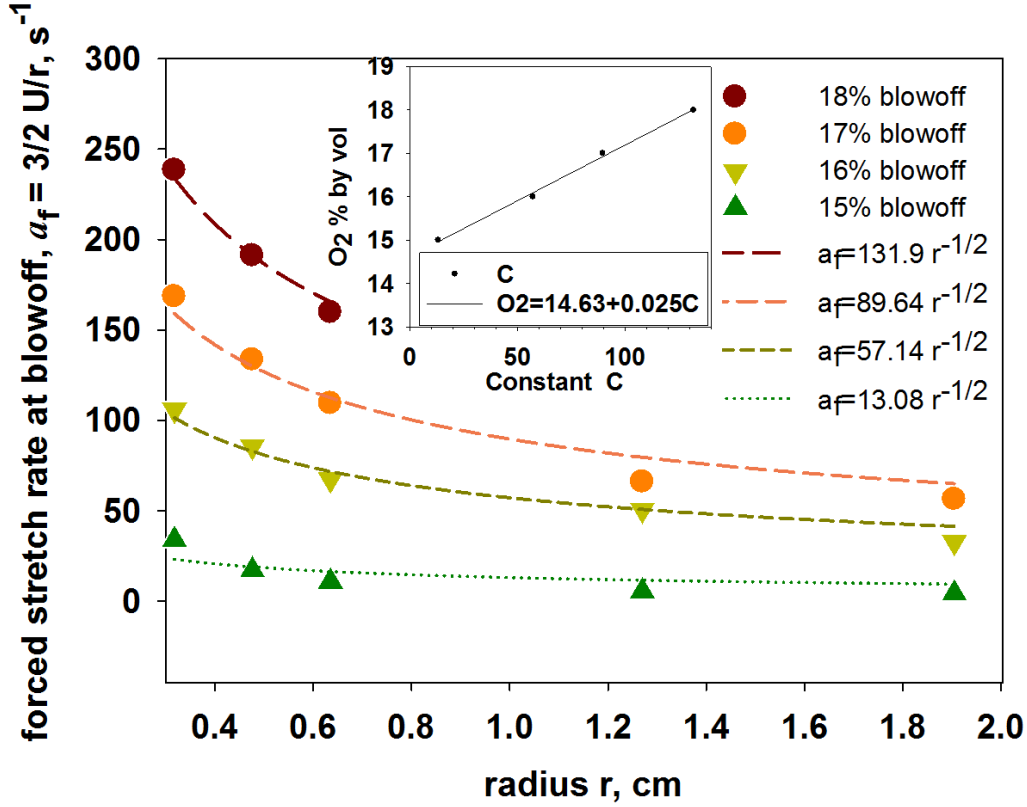


**Figure 5:** Forced stretch rate at blowoff plotted against rod radius at each oxygen concentration. The inset shows the constant of each power law curve fit, which varies linearly with oxygen.

To collapse the data at different radii into a single blowoff boundary, the flame curvature needs to be accounted for, so for a given flow speed we introduce the normalized thermal length ratio  $\delta/\delta_o = (r/r_o)^{1/2}$  discussed above where  $r_o$  is the smallest rod radius = 0.318 cm. In addition, the flow acceleration in the quartz tube due to the presence of the rod becomes significant for the larger rod sizes, as noted by [15]. To account for this flow acceleration, a blockage factor was defined as  $B = A_{tube}/(A_{tube} - A_r)$  as follows:

$$U_{tube} A_{tube} = U_{accel} (A_{tube} - A_r)$$

$$U_{accel} = \frac{U_{tube} A_{tube}}{(A_{tube} - A_r)} = B U_{tube}$$

Where  $U_{tube} = U$  in the stretch rate definition, and  $A_{tube}$  and  $A_r$  are the cross-sectional areas of the tube and rod, respectively. Table 1 shows the  $B$  values for each  $r$ .

**Table 1: Blockage factor B for each rod radii**

r, cm	A <sub>r</sub> , cm <sup>2</sup>	A <sub>tube</sub> , cm <sup>2</sup>	B
0.318	0.318	45.604	1.007
0.476	0.712	45.604	1.016
0.635	1.267	45.604	1.029
1.270	5.067	45.604	1.125
1.905	11.401	45.604	1.333

Using these corrections, an adjusted forced stretch rate  $a_o$  is defined as

$$a_o = \left[ \frac{3U}{2r} \right] * \left[ \frac{A_{tube}}{(A_{tube} - A_r)} \right] * \left[ \frac{r}{r_o} \right]^{1/2}$$

The blowoff data from Figures 3 and 5 is replotted using the adjusted forced stretch rate as the x-axis in Figure 6. The data collapses into a single blowoff boundary for all the normal gravity data. The BASS-II flammability boundary [12] is also plotted in Figure 6. There is a clear offset between the normal gravity data and the microgravity data. An empirical linear superposition of the buoyant stretch rate of  $a_b=78 \text{ s}^{-1}$  is used to align the data with the BASS-II boundary ( $a_{total} = a_o + a_b$ ). For the smallest rod size, this is an effective forced flow of 16.5 cm/s, in good agreement with normal gravity buoyant flow velocities ( $\sim 20 \text{ cm/s}$ ) [16]. The linear fit to the shifted data is given by the blue-shaded band. This blowoff region is inherently wide due to the stochastic nature [18] of the blowoff limit.

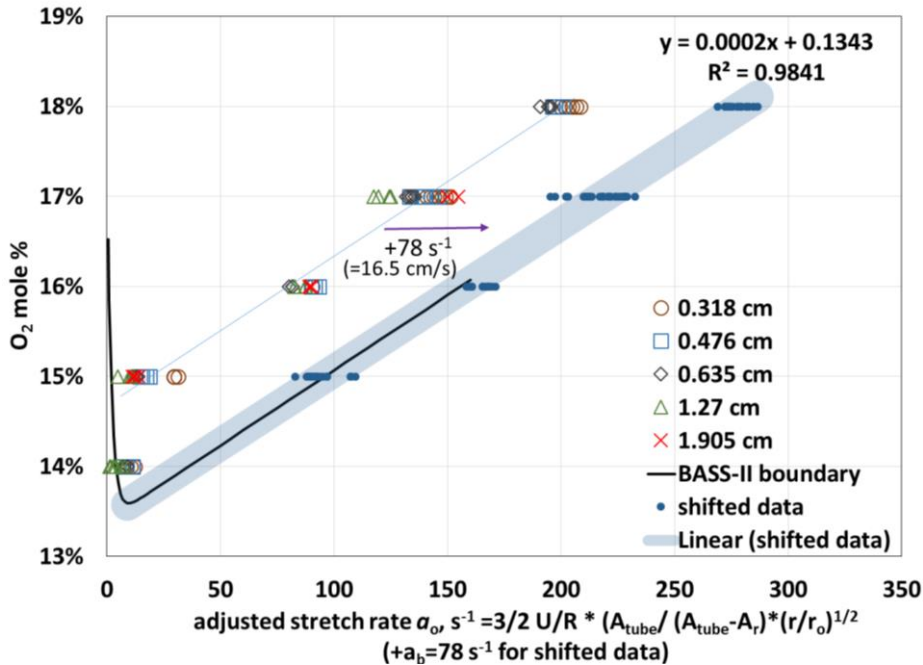


**Figure 6:** Blowoff boundary correlation that accounts for the flow acceleration due to rod blockage in the quartz tube, and normalizes all the radii to the smallest radius  $r_o$  using the gas phase length scale  $\delta$ . To account for buoyant stretch, a shift of  $78 \text{ s}^{-1}$  aligns the normal gravity data with BASS-II data [12]

The linear trend in blowoff data with oxygen is noteworthy and potentially useful for developing an improved test method that can be performed in normal gravity to determine flammability in microgravity. The idea is that the actual flammability boundary as given by the BASS-II data can be approximated simply by the extrapolating the linear blowoff boundary to zero stretch, which estimates that 13.4% O<sub>2</sub> is the limiting oxygen concentration below which the fuel cannot burn at any stretch rate. From a fire safety aspect, it is a conservative estimate but still quite close to the observed 13.6% O<sub>2</sub> minimum concentration needed to get stable flames in BASS-II [12]. The estimate is good because the microgravity quenching boundary turns upward away from the blowoff line only for low-speed flows, a very narrow region (compared to the overall boundary).

The use of an empirical shift to determine the buoyant stretch predicates knowledge of the microgravity boundary, which is not generally the case. Using another way to account for the shift, consider the formulation from [17] where the buoyant stretch takes the form

$$a_b = K \sqrt{\frac{g}{r}}$$

Using values  $a_b = 78 \text{ s}^{-1}$ ,  $g = 981 \text{ cm/s}^2$ , and  $r_o = 0.318 \text{ cm}$ , the constant  $K$  is estimated to be 1.4. Further research is needed to determine the applicability of the buoyant stretch constant  $K$  for different materials. Since  $K$  is a density ratio [17], and gas-phase chemistry at the blowoff limit may have the same limiting reaction rate for a given flow rate (critical Damkohler number), the critical temperatures may be similar for different materials with the same basic gas phase chemistry [1] at each oxygen concentration. Thus for common C-H-O fuels one would expect the density ratio to also be similar at blowoff. On the other hand, fuels with other chemical additives (N, Br, Cl, P, etc.) may not follow the same trends.

#### 4. Conclusions

Normal gravity blowoff limits were measured for the axisymmetric cast PMMA rod geometry in upward axial stagnation flow. Five radii (0.318 cm to 1.905 cm) at five oxygen concentrations (14 to 18% by volume) were tested. The blowoff velocities were converted to forced stretch rates. By using a normalized thermal length ratio  $\delta/\delta_o = (r/r_o)^{1/2}$  to account for the stretch rate at the flame standoff distance and normalizing the results to the base rod size as well as adjusting the flow due to rod blockage in the tube, all the data was correlated onto a single curve.

The blowoff boundary in normal gravity was compared to the complete microgravity extinction boundary from the Burning and Suppression of Solids – II (BASS-II) experiments performed aboard the International Space Station. The normal gravity blowoff boundary was parallel to the BASS-II boundary, but shifted to lower stretch rates. In order to account for the additional inherent buoyant stretch, the normal gravity boundary was empirically shifted to the right by a value  $a_b = 78 \text{ s}^{-1}$ , which for the base rod size corresponds to a forced flow velocity of 16.5 cm/s, in good agreement with buoyant flow velocity estimates.

We suggest an improved normal gravity ‘upward flame spread test’ method to estimate material flammability in microgravity. The first step is to determine the normal gravity blowoff boundary for an axisymmetric rod geometry burning in a forced flow tube. Then, the buoyant stretch contribution is added to predict the microgravity blowoff boundary. Further research is



needed to determine the applicability of the buoyant stretch constant  $K$  for different materials. If proven for various materials, this linear boundary, extrapolated to zero stretch, could provide a conservative estimate of flammability limits in microgravity. The technique may work for a wide range of materials as long as the extinction boundaries have a similar shape. This test method may improve spacecraft fire safety for future exploration missions.

## 5. Acknowledgements

The ISS Research Project Office funded this work. The authors want to acknowledge the personnel from the NASA Glenn Zero Gravity Research Facility, led by Professional Engineer Eric Neumann, for their assistance in preparation of the rod samples, design and fabrication of the flow straightener and flow system, and support of supplemental wind tunnel normal gravity testing at 14% oxygen. The authors would also like to thank Jay Owens for his help in setting up the camera control system for normal gravity testing.

## 6. References

- <sup>1</sup> R.F. Simmons, H. G. Wolfhard, *Combust. Flame* 1 (2) (1957) 155-161.
- <sup>2</sup> A. Linan, *Acta Astronautica* 1 (1974) 1007-1039.
- <sup>3</sup> S.H. Sohrab, A. Linan, F.A. Williams, *Combust. Sci. Tech.* 27 (1982) 143-154.
- <sup>4</sup> J.S. T'ien, H. Bedir, *Proc. Of 1st Asia-Pacific Conference on Combust.* (1997) 12-15.
- <sup>5</sup> J.S. T'ien, *Combust. Flame*, Vol. 65 (1986) 31-34.
- <sup>6</sup> J.S. T'ien, *Progress in Scale Modeling* (2008) 281-292.
- <sup>7</sup> L. Krishnamurthy, *Combust. Sci. Tech.* 10.1-2 (1975): 21-25.
- <sup>8</sup> H. Tsuji, *Progress in Energy and Combustion Science*, 8(2) (1982) 93-119.
- <sup>9</sup> Y. Halli, J. S. T'ien, NBS-GCR-86-507 (1986).
- <sup>10</sup> S. L. Olson, Case Western Reserve University Dissertation, May, 1997.
- <sup>11</sup> C. Sanchez-Tarifa, B. Lazaro, *Microgravity Research and Applications in Physical Sciences and Biotechnology*, 454 (2001), 267-274.
- <sup>12</sup> S.L. Olson, P.V. Ferkul, 9th U. S. National Combustion Meeting, The Combustion Institute, May 17-20, 2015, Cincinnati, Ohio.
- <sup>13</sup> V. Nayagam, R. Balasubramanian, P.D. Ronney, *Combust. Theory Modelling* 3 (1999) 727-742.
- <sup>14</sup> S.L. Olson, F.J. Miller, *Proc. Combust. Inst.* 32 (2009) 2445-2452.
- <sup>15</sup> H. Tsuji, I. Yamaoka, *Proc. Combust. Inst.* 11 (1967) 979-984.
- <sup>16</sup> H.D. Ross, ed. Microgravity Combustion, Academic Press (2001) 313-329.
- <sup>17</sup> S.L. Olson, J.S. T'ien, *Combust. Flame* 121 (2000) 439-452.
- <sup>18</sup> J. S. T'ien, *Combust. Sci. Tech.* 7 (1973) 185-188.